The 2013 World Congress on
Advances in Structural Engineering and Mechanics (ASEM13)
Jeju, Korea, September 8-12, 2013

Effect of beam dimensions on structural performance of wide beam-column joints

J.S. Kuang[1)] and *Wing Shan Kam[2)]

[1), 2)] *Department of Civil and Environmental Engineering, Hong Kong University of Science and Technology, Hong Kong*
[2)] wskamaa@ust.hk

ABSTRACT

The structural performance and cyclic behaviour of reinforced-concrete wide beam-column joints are studied by computational simulations with ABAQUS. Five wide beam-column joint specimens with the same column sizes but different beam widths and beam depths are simulated. Implicit finite element analyses are conducted, where concrete and steel reinforcement are modelled with 8-note 3-D solid elements and 2-node 3-D truss elements, respectively. The studies focus on the effects of beam widths and beam depths on the load transfer paths. It is shown that lesser crack opening occurs in wide beam-column connections; hence less pinched hysteresis loops are observed. The beam width has significant effect on the load transfer paths in wide beams and the corresponding joint cores. The simulated results also indicate that joint shear stress in wide beam-column connections is higher than that of conventional ones.

1. INTRODUCTION

Wide beam systems in buildings may reduce the amount of formwork through repetition and then the construction cost can be greatly reduced and the construction works can be simplified. On the other hand, smaller storey height can be achieved from a wide beam system due to shallow beam depths. However, the performance of wide beam structures subjected to seismic loads is not well understood since only limited experimental results are available.

Shear transfer in a reinforced concrete, wide beam-column joint is a rather complex mechanism, in which the force transfer may be through the formation of a concrete strut-and-tie mechanism in the inner portion of the beam, while the wide beam moment is transferred to the column through torsion in the remaining parts on the two sides. This load transfer path in a wide beam-column joint is in fact still not well understood due to only a limited number of research works done on wide beam-column joints (LaFave and White 2001; Benavent-Climent et al. 2009, 2010). Codes of practice in various countries have provided different recommendations on the use of wide

[1)] Professor
[2)] MPhil Student

beam-column systems by limiting the beam width. In EC-8, the width of the beam is limited to the lesser of b_c+h_b and $2b_c$, whereas ACI 318-08 limits the width of the beam to the lesser of $b_c+1.5h_c$ and $3b_c$, where b_c is the column width, h_b is the beam depth and h_c is the column depth respectively. In general, the structural parameters that are vital in affecting the load transfer mechanisms in wide beam-column joints include the beam-to-column width ratio, beam depth and column depth.

This paper presents computational simulations of the structural performance of reinforced concrete wide beam-column joints with different beam widths and beam depths. The studies focus on the effects of beam width and beam depth on the load transfer path in wide beam-column joints as well as on the hysteresis behaviour of the joints, where five RC beam-column joint models are built and analysed using ABAQUS.

2. FINITE ELEMENT MODELLING

2.1 Prototype models

In the study, five specimens of wide beam-column joint assembly are simulated, which have the same column size of 300×500 mm (b_c×h_c) but different beam widths and beam depths. Geometry and reinforcement details of the prototype models are shown in Table 1. It can be seen that specimen A is a conventional beam-column joint, while specimens B to E are wide beam-column joints. These specimens represent typical exterior wide beam-column connections in moment-resisting RC frame buildings, constructed based on the assumption that the points of contraflexure are located at mid-span of beams and mid-height of columns.

Table 1 Geometry and reinforcement details of specimens

Specimen	A	B	C	D	E
Main beam b_b×h_b (mm)	300×300	600×300	900×300	600×400	900×400
Main beam flexural steel ratio	1.40%	1.22%	0.93%	0.93%	0.70%
Main beam stirrup	R10@100	R10@100 in pairs			
Column size b_c×h_c (mm)	300×500				
Column steel ratio / stirrup	3.93% / R10@100 in pairs				
Transverse steel in joint core	3T16 hoops				
Transverse beam b×h (mm)	500×300			500×400	

2.1 Element Types

In the finite element analysis, concrete is modelled with linear 8-nodes, 3-D solid elements (C3D8R). The reduced integration approach is adopted to eliminate the locking behaviour resulted from the first-order elements, and the enhanced hourglass control is applied to suppress the zero-energy modes resulted from the reduced integration. Steel reinforcement is modelled with 2-node,3-D truss elements (T3D2), which is fully embedded in concrete, such that the concrete can effectively constrain the translational degrees of freedom of embedded nodes of the steel. After carrying out

mesh sensitivity studies, average mesh size of 160 mm is adopted for the finite element models, as shown in Fig. 1.

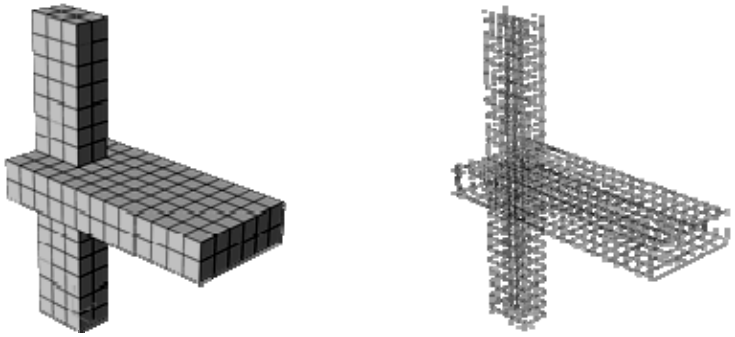

Fig. 1 Finite element model of specimens

2.2 Constitutive models of concrete and steel reinforcement

The constitutive model adopted for concrete is the damage-plasticity model for quasi-brittle materials (Lubliner et al. 1989; Lee and Fenves 1998). This model composes of the concept of non-associated multi-hardening plasticity and makes use of isotropic damaged elasticity as well as isotropic tensile and compressive plasticity to characterise the non-linear, irreversible and softening phenomena of concrete subjected to general loading. The yield function in the model is defined as

$$F(\bar{\sigma}, \tilde{\varepsilon}^{\text{pl}}) = \frac{1}{1-\alpha}(\bar{q} - 3\alpha\bar{p} + \beta(\tilde{\varepsilon}^{pl})\langle\hat{\bar{\sigma}}_{\max}\rangle - \gamma\langle-\hat{\bar{\sigma}}_{\max}\rangle) - \bar{\sigma}_c(\tilde{\varepsilon}^{pl}) \quad (1)$$

Where $\bar{p}$ and $\bar{q}$ are the effective hydrostatic stress and Mises equivalent effective stress, respectively; $\bar{\sigma}_c$ is the algebraically maximum eigenvalue of effective stress tensor; and and are the parameters that control the shape of the yield surface in stress space. The flow rule is non-associated and the flow potential is taken as Drucker-Prager hyperbolic function,

$$G = \sqrt{(e\sigma_{t0}\tan\varphi)^2 + \bar{q}^2} - \bar{p}\tan\varphi \quad (2)$$

where φ is the dilation angle measured in the p–q plane at high confining pressure; σ_{t0} is the uniaxial tensile stress at failure; and e is the eccentricity defining the rate at which the function approaches the asymptote so that the flow potential tends to linear Drucker-Prager flow potential as the eccentricity tends to zero. The stress-strain relationships for concrete in both tension and compression were modelled based on the CEB-FIP Model Code. In addition, fracture energy in tension and compression are introduced as material parameters in order to tackle the mesh sensitivity and localization issues in the numerical simulations (Krätzig et al. 2004). In the study, the grade C40 concrete is used and the material parameters of the concrete are obtained from the CEB-FIP Model Code. Damping was also considered in the properties of concrete,

where Rayleigh damping coefficients of each specimen are determined by the frequency analysis using ABAQUS.

The smeared stress-strain relationship required in the fixed angle soften truss model (Hsu and Mo 2010) is used to determine the properties of steel reinforcement, which is a bilinear model. The yield stress of all flexural steel bars and shear stirrups at beam-column joint cores is 500 MPa, while that of other shear reinforcement is 250 MPa. The average stress and strain are given by

$$f_s = E_s \varepsilon_s \quad (\varepsilon_s \le \varepsilon'_y) \tag{3a}$$

$$f_s = (0.91 - 2B) f_y + (0.02 + 0.25B) E_s \varepsilon_s \quad (\varepsilon_s > \varepsilon'_y) \tag{3b}$$

where $_s$ is the smeared steel strain, f_s is the smeared steel stress, $'_y$ is the average yield strain of steel embedded in concrete, given by $\varepsilon'_y = (0.93 - 2B) f_y / E_s$, and B is a parameter defined by $B = (1/\ )(f_{cr}/f_y)^{1.5}$, in which is the reinforcement ratio.

2.3 Applied Load

The beam end is supported by a roller while the column base is pinned to the ground. The loading schedule includes two steps. A constant column axial load of 800 kN is first applied. The cyclic lateral displacement is applied at top of the column to simulate the working condition of the beam-column assemblies under load reversals, as shown in Fig. 2.

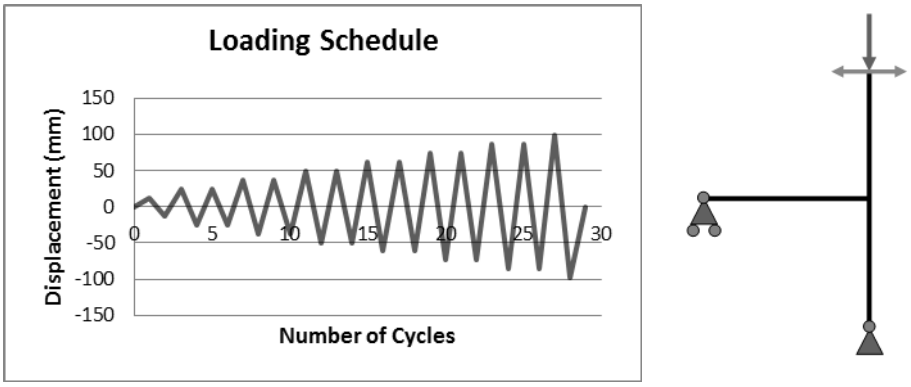

Fig. 2 Boundary conditions and loading schedule

3. SIMULATION RESULTS

3.1 Effect of beam width

The hysteretic loops of specimens A, B and C are presented in Fig. 3. The three specimens have the same beam depth but different beam width, where specimen A is a conventional beam-column joint assembly and specimens B and C are wide beam-column joint assemblies. It is seen that the conventional beam-column joint A exhibits severe pinching hysteresis behaviour and less ductility, as compared with those of the wide beam-column joint specimens B and C. This is because the crack

opening-closing effect takes place extensively in specimen A but not in specimen B and C. In addition, the crack width in specimen A is larger than those in specimens B and C at the same drift ratios. This phenomenon may be due to the difference in orientations of diagonal cracks inside the joint cores. For the conventional beam-column joint, the angle of inclination of diagonal cracks from horizontal axis is deeper than those of wide beam-column joints. In such case, the crack closing effect resulting from the column axial load becomes smaller. Moreover, the well reinforced transverse beams provide additional confining effects to the joint cores to prevent opening of diagonal cracks.

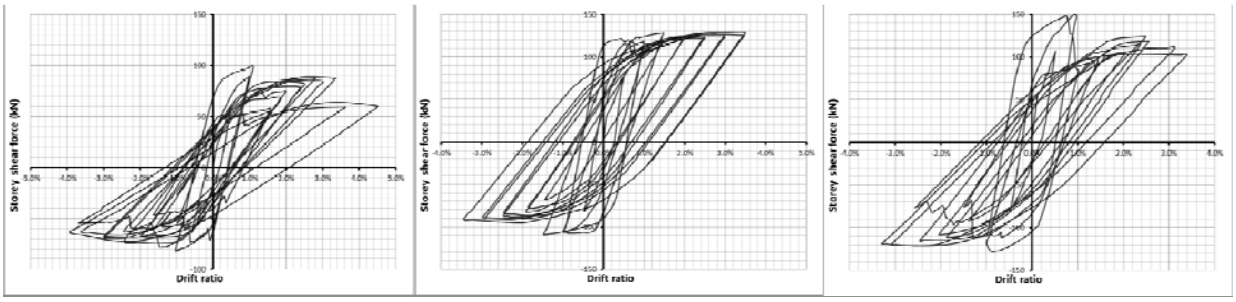

(a) (b) (c)

Fig. 3 Hysteresis loops. (a) Specimen A, (b) Specimen B, (c) Specimen C

It is also seen from Fig. 3 that the beam width has a significant effect on the shear strength of the beam-column joints. The peak strengths of specimens A, B and C are 98.4 kN, 128.7 kN and 149.6 kN, respectively. It is shown that the increase in the beam width can alter the load transfer path from beam to joint core, thus enhancing the beam-column joint assemblies and result in the higher peak strength. However, when the width of the wide beam increases, there is early stiffness degradation and the pinching effect becomes more obvious by comparing wide beam specimens B and C.

When the failure of specimens occurred, the largest plastic deformations are observed at the joint core and the longitudinal beam bars are yielded. However, the steel reinforcement at the inner part of the beam shows a larger plastic strain than those at the outer part of the beam. In specimen B and D, where the beam width is 600 mm, all the longitudinal beam bars close to the joint have similar plastic strains, though the plastic strain in the outermost reinforcing bars is slightly lower than that in the inner ones. This phenomenon is much more obvious in specimens C and E, which have the same beam width of 900 mm. The plastic strain in the outermost reinforcing is only around 20% of that in the inner ones. Therefore, the outer portion of the beam should not be considered as part of the joint, i.e. the effective beam width should be taken as less than the actual beam width.

3.2 Effect of beam depth

The hysteretic loops of specimens D and E are presented in Fig. 4. By comparing Figs. 5(a) to 3(b) and 5(b) to 3(c), it can be seen that a wide beam-column joint with larger beam depth performs better and achieves higher shear strength than the joint that has the same beam width but the smaller beam depth.

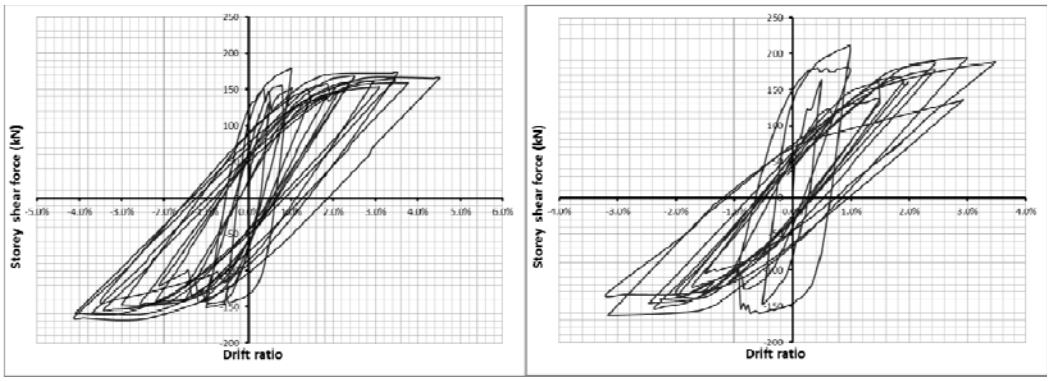

(a) (b)

Fig. 4 Hysteresis loops. (a) Specimen D, (b) Specimen E

Fig. 5 shows the load transfer paths in a wide beam-column joint. It is seen that because the compression strut with an angle of about 30° to the z-axis in formed, the increase in the beam depth leads to the indirect increase in the effective beam width, thus enhancing the shear strength of the joint.

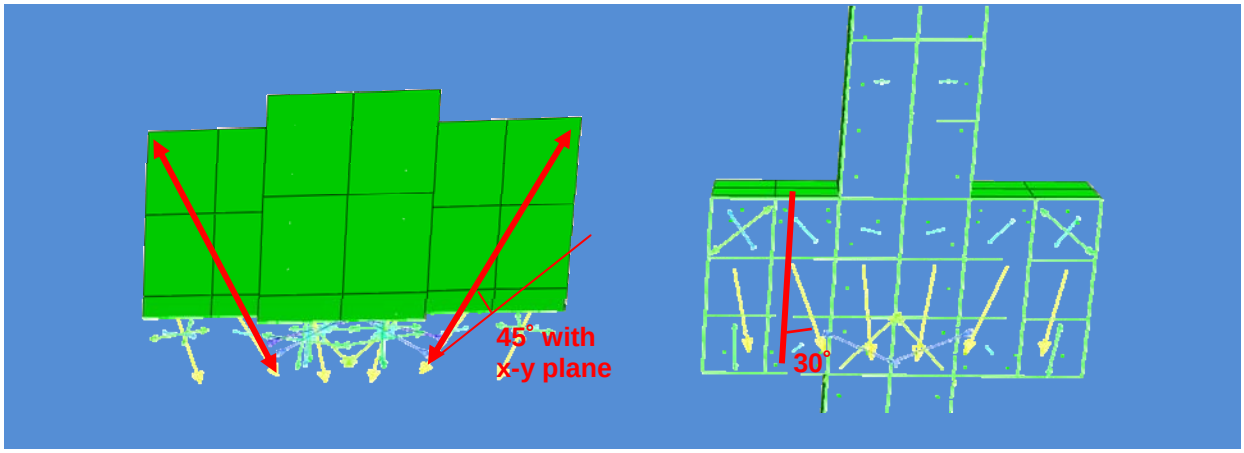

Fig. 5 Load transfer paths in wide beam-column joint E

4. CONCLUSIONS

The structural performance and cyclic behaviour of reinforced-concrete wide beam-column joints are studied by computational simulations with ABAQUS. Five wide beam-column joint specimens with the same column sizes but different beam widths and beam depths are simulated. Implicit finite element analyses are conducted. Based on the results from computational simulations, the following conclusions can be drawn.

1. The beam to column width ratio has the significant effect on the cyclic behaviour of a wide beam-column joint, since the load transfer paths in wide beams depend largely on the width of the beam. The loads from a wide beam are first transferred to the

connected transverse beam and then to the joint. A wide beam with very large beam width may induce significant torsion in the transverse beam, thus causing the adverse effect on the joint.

2. For wide beam-column joint assemblies, the increase in beam depth may lead to a direct load transfer from wide beam to beam-column joint core through an about 30˚ comprssion strut. A larger width of the beam will then participate in trasferring loads directly to the joint.

3. By considering the effects of both the beam-to-column width ratio and the beam depth, the effective beam width of RC wide beam-column joints may be limited to the lesser of b_c+h_b and $2b_c$ in design practice, which is the same as that recommended by EC-8.

ACKNOWLEDGEMENT

The support of the Hong Kong RGC under grant No. 614011 is gratefully acknowledged.

REFERENCES

Benavent-Climent, A., Cahís, X. and Vico, J.M. (2010), "Interior wide beam-column connections in existing RC frames subjected to lateral earthquake loading," *Bull Earthq Eng*, **8**, 401–420.

Hsu, T.T.C. and Mo, Y.L. (2010), *Unified Theory of Concrete Structures*, Wiley, New York.

Krätzig, W.B. and Pölling, R. (2004), “An elasto-plastic damage model for reinforced concrete with minimum number of material parameters,” *Comp Struct*, **82**, 1201-1215.

LaFave, J.M. and Wight, J.K. (2001), “Reinforced concrete wide beam-column connections vs. conventional construction: Resistance to lateral earthquake loads,” *Earthq Spectra*, **17**, 479-505.

Lee, J. and Fenves, G.L. (1998), “Plastic-damage model for cyclic loading of concrete structures,” *J Eng Mech ASCE*, **124**, 892–900.

Lubliner, J., Oliver, J., Oller, S. and Onate, E. (1989), “A plastic-damage model for concrete,” *Int J Solids Struct,* **25**, 229-326.